UDC 539.4

Analysis of Viscoelastoplastic Behavior of Expanded Polystyrene under Compressive Loading: Experiments and Modeling

A. Imad,[a] A. Ouâkka,[b] K. Dang Van,[b] and G. Mesmacque[c]

[a] Laboratoire d'Etudes des Structures, Ecole des Hautes Etudes Industrielles, Lille, France

[b] Laboratoire de Mécanique du Solide, Ecole Polytechnique, Palaiseau, France

[c] Laboratoire de Mécanique de Lille, Lille, France

УДК 539.4

Анализ вязкоупругопластического поведения растянутого полистирена при сжатии: эксперименты и моделирование

А. Имад[а], А. Уакка[б], К. Данг Ван[б], Г. Месмакю[в]

[а] Лаборатория изучения структуры, Лилль, Франция

[б] Лаборатория механики твердого тела, Паласо, Франция

[в] Лаборатория механики, Лилль, Франция

При использовании расширенного полистирена в случае прокладки дорог, когда почва имеет особые свойства (например, сжатое состояние), возникает необходимость изучения механических характеристик этого материала. В данной работе исследованы механические свойства расширенного полистирена при сжатии. Работа включает две части: экспериментальное исследование и моделирование.

Экспериментальные данные показали, что поведение расширенного полистирена при сжатии характеризуется тремя стадиями. При анализе установлено, что плотность расширенного полистирена играет важную роль.

Рассмотрена феноменологическая механическая модель для моделирования вязкоупругопластических свойств при сжатии. С помощью численного анализа описаны механические свойства, которые хорошо согласуются с полученными экспериментально.

Ключевые слова: расширенный полистирен, сжатие, вязкоупругопластическое поведение.

Introduction. Expanded polystyrene (EPS) is manufactured from expandable polystyrene beads, which are fused and moulded in moulds using dry saturated steam [1]. The final product is the low-density EPS foam. It has a closed cell structure, wherein 95% of the volume is occupied by air. The specific density of polystyrene, equal to 1050 kg/m^3, is reduced to the range 8 to 60 kg/m^3 depending on the type of EPS [2–3]. Thus, EPS is a highly porous material, which contains 1.15 to 3.25% of polymer and has a complex structure that can be decomposed into two basic elements [2–5]: beads and cells (Fig. 1). The geometry of cells can be defined by their mean diameter (cellularity) (c) and wall thickness (e). Microscopic observations reveal that cell walls contain

microporosity [12]. Beads are simply defined by their mean diameter (granulometry) (g). Beads and cells present structural isotropy that can also be seen on macromechanical level. The EPS structure can be described by three geometrical parameters, namely, $g, c,$ and e that can vary significantly within an EPS block. Moreover, there is no direct correlation between those parameters and the EPS apparent density ρ^*. However, it can be observed that the e/c ratio that characterizes the compactness of the cells can be linearly correlated with the EPS density by the following equation [7, 12]:

$$\rho^* = 3.47\rho_s \frac{e}{c}, \tag{1}$$

where ρ_s is the PS crystal density (1050 kg/m^3).

In general, this material is frequently used as a packaging material for shock and vibration damping. In this case, cellular materials are usually subjected to high deformation rates and their mechanical behavior under dynamic compression plays an important role, as well as their energy absorption characteristics [11, 15].

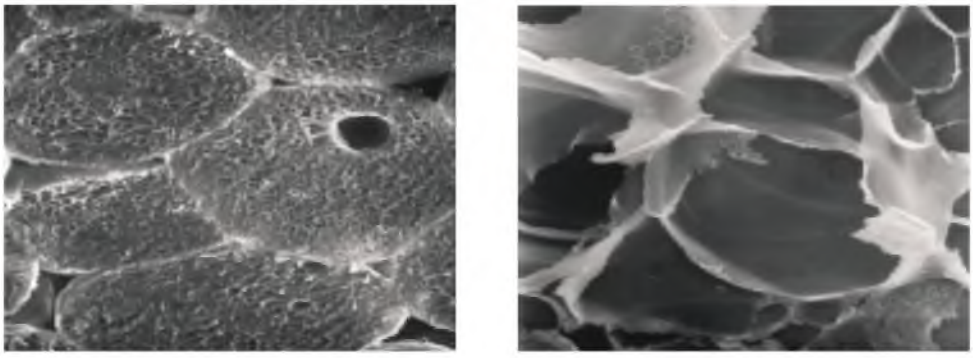

a *b*

Fig. 1. Expanded polystyrene microstructure: beads (*a*) level and cells (*b*) level.

Recently, EPS has also been used as lightweight fill for sub-road pavement for compressible or unstable soils [1–3]. This application leads researchers to study EPS mechanical behavior under static compressive or creep loading at low deformation rates [4–7]. These works, essentially experimental, allow a better understanding of the EPS behavior and establishing empirical models relating the EPS mechanical properties to its relative density [5–7]. These relationships are similar to those usually used for traditional foams [8–11].

The mechanism of the EPS compression is the addition of two simultaneous phenomena:

– cell walls, solid polymer compression;

– cell enclosed, air compression.

For this purpose, the EPS compressive mechanical behavior has been analyzed using a global approach. This work consists of experimental and numerical studies based upon a rheological model and finite-element simulation.

1. **Experimental Procedure**. Specimens were machined using a hot wire process and have the shape of a parallelepiped ($L = 100$ mm, $H = 75$ mm, and $l = 100$ mm). Compression tests were conducted under environmental conditions at a constant crosshead displacement speed (4 mm/min). Five samples were tested for each EPS density in order to obtain the mean mechanical behavior [12, 17]. Because of density variation inside an EPS block, the density of each specimen was measured prior to the test, giving the apparent density value ρ^*. The density of specimens was determined from their weight and dimensions. In this investigation, eighteen types of the EPS were tested corresponding to three density values (15, 20, and 30 kg/m^3) and different sizes of the cells and beads. Globally, the density varies from 13 to 37 kg/m^3 [12].

2. **Results and Discussion**. Compression causes transverse deformation leading to Poisson's ratio nearly equal to zero [8]. This results in an increase in the apparent density ρ^* with the applied strain: compressibility of the material (Fig 2). The above observation is similar for all cellular materials [11]. This mechanical behavior leads to an increase in the apparent density with the longitudinal strain ε, according to the following expression:

$$\rho^* = \rho_0^* \left(\frac{1}{1-\varepsilon} \right), \tag{2}$$

where ρ_0^* is the initial apparent density of the material and ε is the applied strain under compressive loading.

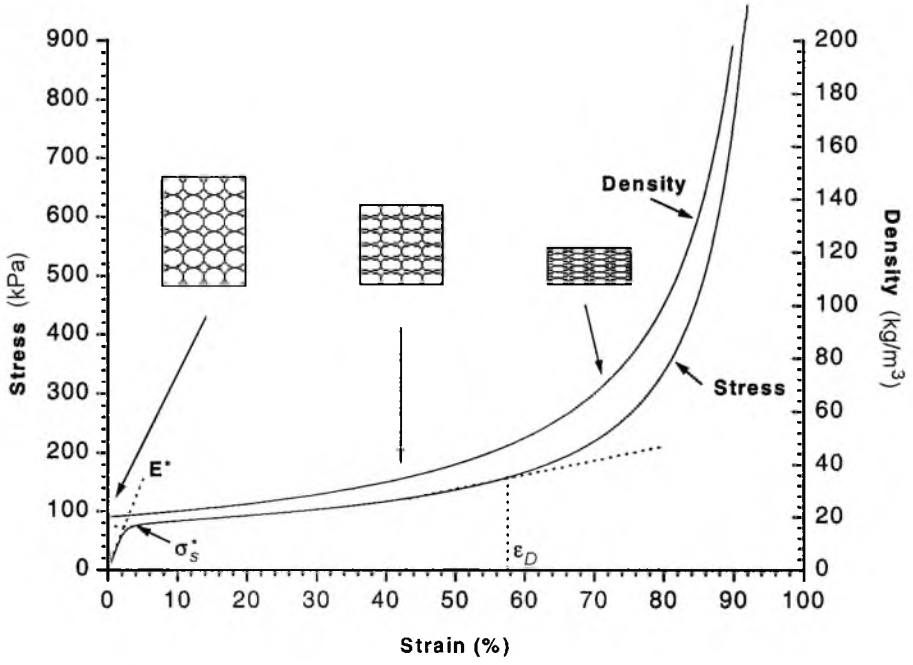

Fig. 2. Stress and density vs strain.

Figure 2 presents a complete EPS compressive stress-strain curve, which is typical of all cellular materials. It is linear-elastic up to 4% strain. This portion is determined by the tangent modulus E^*. The plastic phase is represented by a horizontal plateau, which extends to about 60% strain and is characterized by the yield stress σ_s^*. When the specimen is essentially composed of the polymer, the stress increases rapidly. This final phase is defined by the densification strain ε_D. Most foams have a typical sigmoid stress-strain relationship that can be described by a variety of empirical models [11, 19].

The value of the yield stress σ_s^* can be obtained either from experimental tests, from residual strain analysis using "loading–unloading" technique or recovery tests, and graphically (Fig. 3); σ_s^* is the stress value corresponding to the intersection of the initial tangent and plateau tangent (Fig. 2) [11, 19].

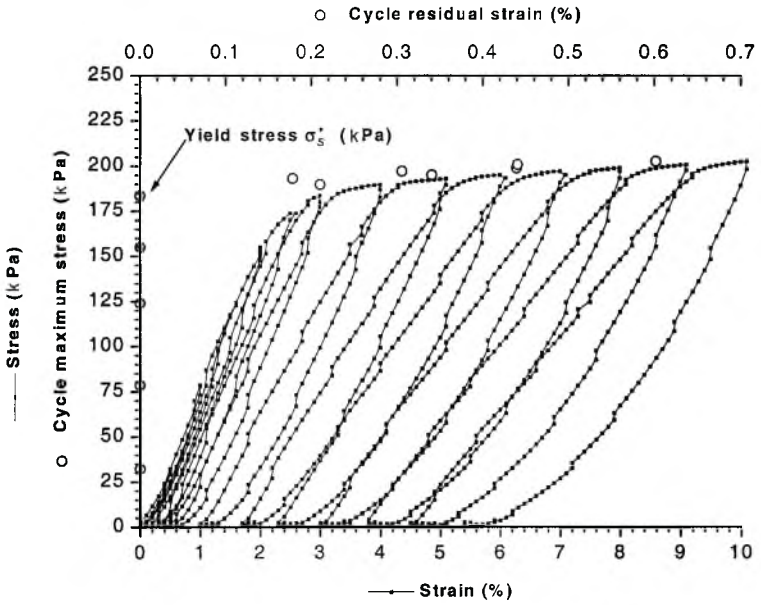

Fig. 3. Determination of the yield stress value: stress vs strain and cycle maximum stress vs cycle residual strain.

A preliminary study was performed in order to verify the uniformity of compressive deformation in the axial direction. For this purpose, a sample was marked with seven lines along the longitudinal dimension L. The distance between those lines was equal to b (Fig. 4). The variation of the displacement value during a compression test was measured using image analysis in order to determine the value of Δb. The local strain calculated by the ratio $\Delta b / b$ was compared to the global strain determined by the ratio $\Delta L / L$. Figure 4 illustrates the local and global strains and shows that these strains are similar. This observation indicates that the global measure of displacement is sufficient for the determination of the applied strain in order to realize the stress-strain curve. For many types of foams, directly under the applied load, the cell structure appears to bend and buckle. Damage to the entire specimen is done in a progressive way.

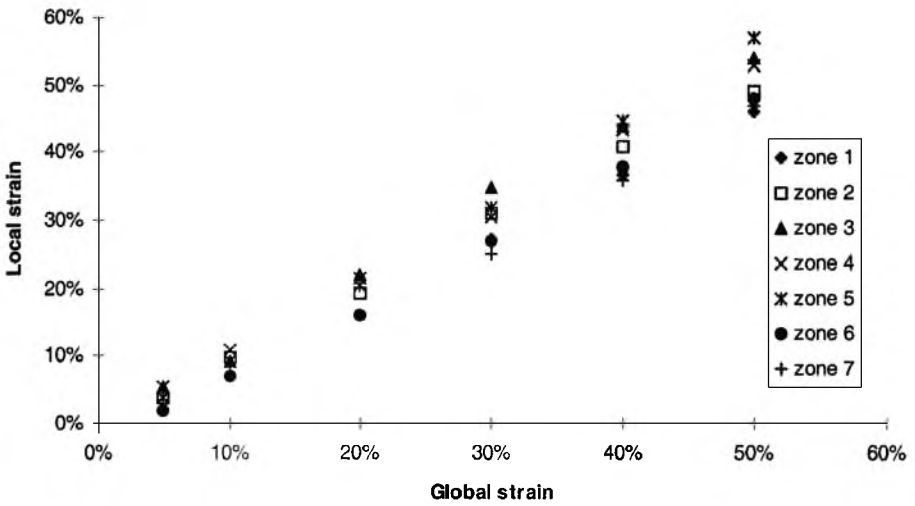

Fig. 4. Local sample deformation vs global sample deformation.

Compression tests were conducted in order to study the influence of the strain rate. The displacement rates studied were 1, 2, 4, 5, 10, 20, 30, 50, and 100 mm/min. The results obtained show that an increase in the displacement rate leads to a slight increase in the yield stress and has no effect on the tangent modulus (Fig. 5). These results are similar to those published for cellular materials [11]. The slight yield-stress increase is caused by the viscous behavior of the material. Actually, at low strain rates, the EPS can adapt itself to the applied stress by air evacuation through the cell-wall porosity. On the contrary, at high-strain rates, the internal cell pressure cannot reach equilibrium. This leads to a slight increase in the sample strength and in the yield stress.

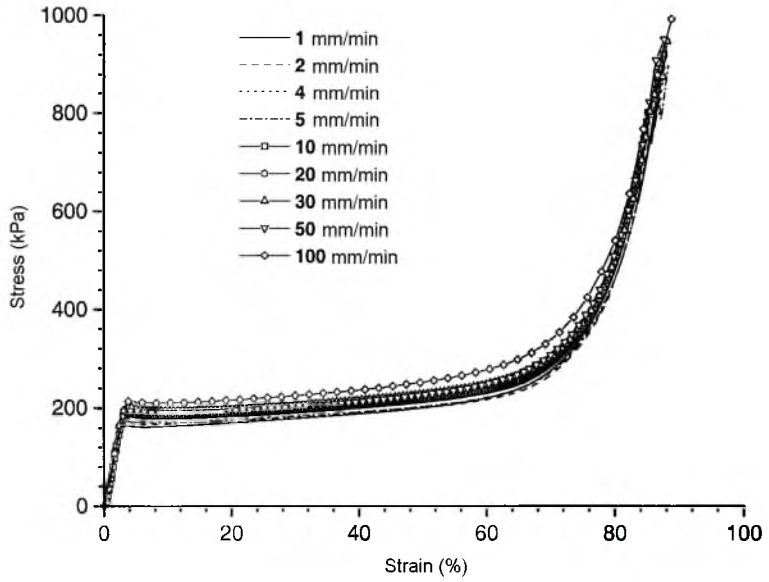

Fig. 5. Crosshead speed influence on EPS compression behavior.

In order to confirm the EPS viscosity, compression–relaxation tests were performed at various strain levels (5, 10, 15, and 20%). The results show a slight viscosity phenomenon whatever the EPS type (a 30% stress decrease). This low viscosity explains the slight strain rate influence on the EPS mechanical behavior (Fig. 6).

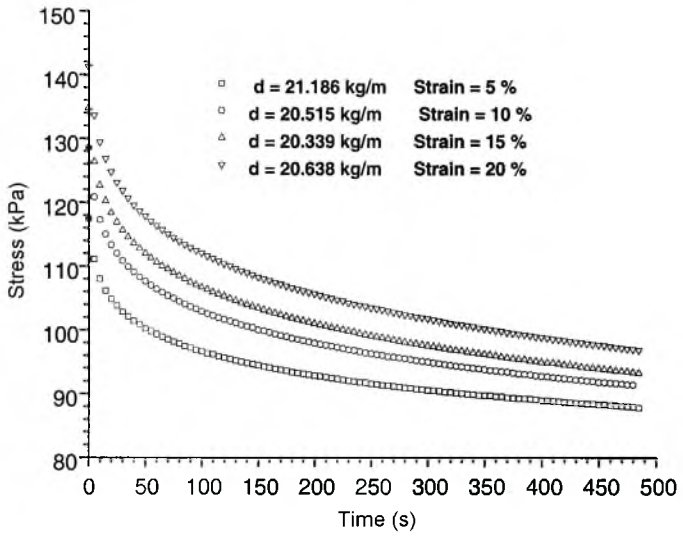

Fig. 6. Stress relaxation.

The apparent density ρ^* is the main parameter, which governs the mechanical behavior of cellular materials [9–11]. In our case, we studied the influence of the EPS apparent density on three mechanical parameters E^*, σ_s^*, and ε_D. The results allowed us to determine empirical relationships between the density and mechanical properties. They are written using the EPS relative characteristics:

$$\frac{E^*}{E_s} = 1.01\left(\frac{\rho^*}{\rho_s}\right)^{1.63}, \tag{3}$$

$$\frac{\sigma_s^*}{\sigma_{s_s}} = 0.37\left(\frac{\rho^*}{\rho_s}\right)^{1.46}, \tag{4}$$

$$\varepsilon_D = 100 - 522.83\frac{\rho^*}{\rho_s}. \tag{5}$$

These relationships show the major density effect on the three mechanical parameters. Indeed, an increase in the relative density leads to an increase in the EPS strength, E^* and σ_s^*, and to a decrease in the densification strain, ε_D (Fig. 7). Generally, the same conclusions have been pointed out in all the cases with cellular materials [11].

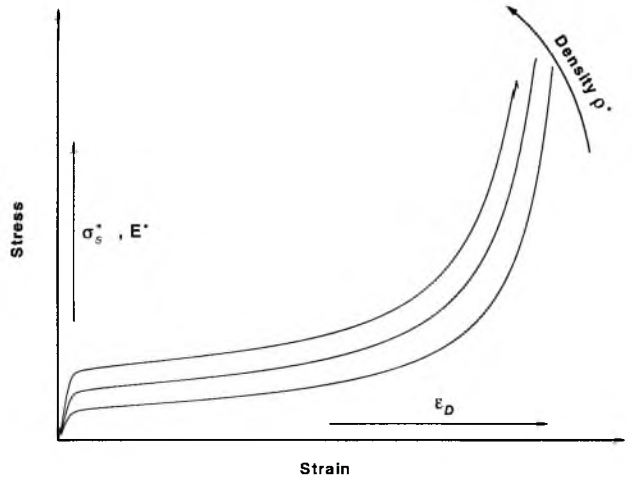

Fig. 7. Influence of density.

3. **Viscoelastoplastic Modeling.**

3.1. *Phenomenological Mechanical Model.* The EPS behavior under compressive loading can be described by rheological models of two particular types of material: the elastoplastic solid and the viscous liquid. Experimental results lead to the conclusion of the EPS viscoelastoplastic mechanical behavior. Here, a global modeling is used in order to simulate the stress-strain curve up to 20% strain. The microstructure of the EPS (beads and cells) is not considered. Indeed, this type of phenomenological mechanical model assumes the existence of an "equivalent material."

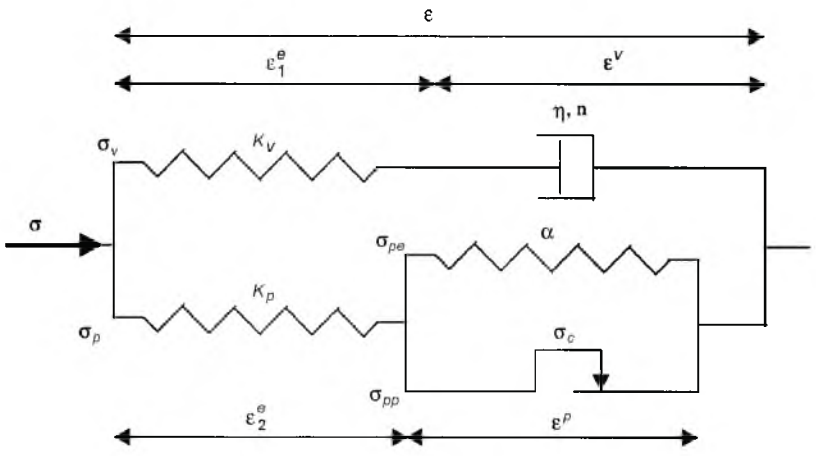

Fig. 8. Rheological model.

The rheological model is built by the superposition of two parallel branches (Fig. 8):

– a viscoelastic branch composed of a spring and a piston assembled in series (nonlinear viscosity). This branch allows simulation of the nonlinear elastic phase and the relaxation mechanism;

– an elastoplastic branch composed of a spring assembled in series with a spring and a pad. This branch allows simulation of the plasticity (pad), densification (spring α) and creep phenomenon (spring K_p assembled with the piston of the viscoelastic branch).

The stress and strain applied to the system come into an elastoplastic and a viscoplastic parts of the model and are given by the following equations:

$$\varepsilon = \varepsilon_1^e + \varepsilon^v = \varepsilon_2^e + \varepsilon^p, \tag{6}$$

$$\sigma = \sigma_v + \sigma_p = \sigma_v + \sigma_{pe} + \sigma_{pp}. \tag{7}$$

The stress–strain relationship for each part of the model are expressed by

$$\sigma_v = K_v \varepsilon_1^e \quad \text{for the } K_v \qquad \text{for the spring,} \tag{8}$$

$$\sigma_v = \eta \left|\dot{\varepsilon}^v\right|^{n-1} \dot{\varepsilon}^v = \eta \left|\dot{\varepsilon}^v\right|^n \operatorname{sign}(\dot{\varepsilon}^v) \qquad \text{for the piston,} \tag{9}$$

$$\sigma_p = K_p \varepsilon_2^e \qquad \text{for the } K_p \text{ spring,} \tag{10}$$

$$\sigma_{pe} = \alpha \varepsilon^p \qquad \text{for the } \alpha \text{ spring,} \tag{11}$$

$$\sigma_{pp} = \sigma_c \qquad \text{for the pad.} \tag{12}$$

This model involves a six parameter set: K_v, η, n, K_p, α, and σ_c. Identification of the parameters has been carried out using a calculation algorithm minimizing the distance between the theoretical and the experimental curves [12, 20, 21]. In this study, the parameters for compression (single identification) and compression–relaxation (multiple identification) tests, are identified.

The error between the theory and the experiment is less than 0.5% for compression tests (Fig. 9) and less than 1.5% for compression–relaxation tests (Fig. 10).

All results for the cases of compression and compression–relaxation are listed in Table 1. These results show that it is possible to relate the experimental values (E^*, ...) and the model parameters K_v, K_p, α, and σ_c. In our case, these relations are expressed by [12]

$$K_p + K_v \approx E^*, \tag{13}$$

$$\frac{\alpha K_p}{\alpha + K_p} \approx \alpha, \tag{14}$$

$$\left[\frac{\sigma_c}{\sigma_s^*}\right]_{\substack{\text{compressive tests}\\ \text{relaxation tests}}} \approx 0.4. \tag{15}$$

Nevertheless, the study of the viscosity parameters η and n shows that there is no correlation with the experimental parameters. Indeed, the viscosity parameters essentially depend on the strain rate, which is constant for the identified tests.

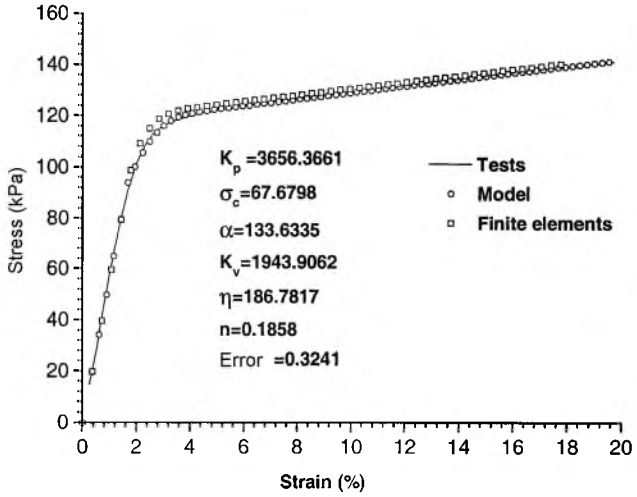

Fig. 9. Stress vs strain: comparison of the rheological and finite-element models and experimental results (compression case).

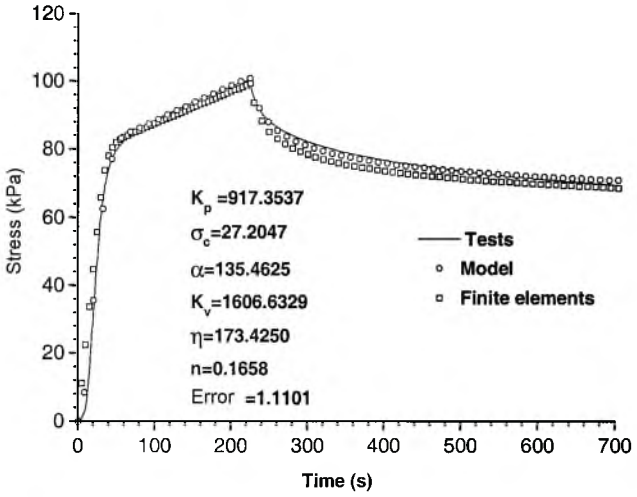

Fig. 10. Stress vs strain: comparison of the rheological and finite-element models and experimental results (compression–stress relaxation case).

It is important to note that the parameters of the rheological model obtained by simple and multiple identifications, are different. This indicates that this type of approach has no unique set of parameters (see Table 1).

T a b l e 1

Parameters of the model values in the compression and compression–relaxation cases

EPS type	K_p	K_v	σ_c	α	η	n	Error (%)
Compression							
A15	1588	879	27	139	466	0.42	0.44
A20	3884	1493	73	214	346	0.30	0.41
A30	6891	7656	93	261	422	0.14	0.29
B15	2523	1041	48	172	216	0.28	0.48
B20	3865	1921	77	259	191	0.19	0.47
B30	7059	5556	132	376	354	0.14	0.46
C15	2194	1220	39	122	154	0.21	0.41
C20	3656	1944	68	134	187	0.19	0.32
C30	3812	3897	62	166	340	0.19	0.37
D15	1728	1262	31	139	223	0.24	0.42
D20	3590	1322	76	27	55	0.06	0.20
D30	5801	7661	41	412	387	0.15	0.58
E15	1986	1278	36	109	210	0.25	0.38
E20	2715	2638	52	142	371	0.24	0.34
E30	2735	5101	44	174	392	0.17	0.37
F15	2312	995	45	100	104	0.18	0.39
F20	3393	2211	65	111	122	0.10	0.32
F30	3827	3216	76	116	206	0.13	0.26
Compression–relaxation							
A15 (10%)	950	1049	20	197	120	0.23	1.02
A15 (15%)	796	1787	15	239	135	0.17	1.25
A20 (15%)	2186	4165	32	296	225	0.15	0.88
A20 (20%)	2247	4378	29	208	235	0.15	1.15
B20 (15%)	1634	4261	26	270	210	0.13	0.96
B20 (20%)	1376	5450	22	229	222	0.11	0.93
C15 (20%)	917	1607	27	135	173	0.17	1.11
D20 (15%)	2218	3548	30	184	184	0.11	0.91
D30 (15%)	3608	3945	86	112	328	0.15	0.51
E20 (20%)	1200	3762	23	140	194	0.11	0.95
E30 (20%)	2667	4375	60	144	306	0.14	0.73
F20 (10%)	1387	4286	24	151	169	0.08	0.81
F20 (15%)	2168	3626	35	106	181	0.11	0.82

The above comments lead to the necessity of finding an experimental procedure to immediately determine the model parameters [12]. This will allow determination of a *sole* parameter set that is not possible using numerical identification.

3.2. *Numerical Modeling.* In this connection, a three-dimensional extension of the rheological equations allows the use of finite-element calculations for the simulation of compression tests. Modeling has been conducted on a quarter of a specimen using a CUB8 element type and Castem 2000 software.

The global mechanical behavior of the EPS foam is considered by using the six identified parameters obtained by the rheological model ($K_v, \eta, n, K_p, \alpha$, and σ_c), which are introduced into the calculation software. Microstructure effects are not considered in this type of modeling. Numerical simulation corresponds to the "equivalent material."

With a uniaxial compressive load applied, the deformation mechanism is similar to experimental observations. The predicted responses of the foam from the finite element analyses were compared to the experimental results.

The results obtained are indeed close to the experimental ones. This allowed us to validate the proposed type of modeling.

Conclusions. The results of studying the EPS compressive loading allow us to draw several conclusions. It has been shown that viscoelastoplastic mechanical behavior of the EPS is affected by a slight viscosity effect leading to almost no strain rate effect. The mechanical parameters describing the elastic and plastic phases, namely, the initial tangent modulus and the yield stress, can be related to the relative density using increasing power laws. The densification strain decreases linearly with a growing relative density. Rheological modeling of compression and compression–relaxation tests has shown that the results are correct and offer confirmation of the EPS viscoelastoplastic behavior. Moreover, finite element simulation using the rheological model parameters and equations allows a correct simulation of compression and compression–relaxation tests. The extension of this approach should make it possible to use numerical calculations for the optimization of the EPS lightweight fill structure.

Acknowledgments. This work was supported by the Hunstman Chemical Company France (HCCF), Ribécourt-France, which produced the EPS material. We would like to thank R. Daffara, B. Beguin, and T. Lucas.

Резюме

При використанні розширеного полістирену у випадку прокладання доріг, коли грунт має особливі властивості (наприклад, стиснення), виникає необхідність у вивченні механічних характеристик цього матеріалу. У даній роботі досліджено механічні характеристики розширеного полістирену при стисненні. Робота складається з двох частин: експериментального дослідження і моделювання.

Експериментальні дані свідчать, що поведінка розширеного полістирену при стисненні характеризується трьома стадіями. Аналіз показав, що щільність розширеного полістирену грає важливу роль.

Розглянуто феноменологічну механічну модель для моделювання в'язкопружнопластичних властивостей при стисненні. За допомогою числового аналізу описано механічні характеристики, які добре узгоджуються з отриманими експериментально.

1. T. A. Coleman, "Polystyrene foam is competitive, lightweight fill," *Civil Engng.*, ASCE, 68–69 (1974).

2. J. P. Magnan and B. Soyez, "Principe des remblais légers; contraintes d'emploi du polystyrène," *Bulletin de Liaison du Laboratoire des Ponts et Chaussées*, Mars–Avril, **136**, 9–13 (1985).
3. J. P. Magnan and J. F. Serratrice, "Proprietes mecaniques du polystyrene expansé pour ses applications en remblai routier," *Bulletin de Liaison du Laboratoire des Ponts et Chaussées*, Novembre–Decembre, **164**, 25–31 (1989).
4. L. J. Gibson and M. F. Ashby, *Cellular Solids, Structures, and Properties*, Pergamon Press, first edition (1988).
5. I. M. Duskov, *Materials Research on Expanded Polystyrene Foam (E.P.S.)*, Delft University of Technology (1994).
6. A. Lefebvre, *Etude du comportement mécanique du polystyrène expansé utilisé en remblais routiers*, D. E. A. de Génie Civil, Hautes Etudes Industrielles, Lille (1994).
7. A. Imad, A. Lefebvre, C. Fornallaz, and B. Beghin, "Etude du comportement mécanique du polystyrène expansé (P.S.E.)," in: *Génie mécanique des caoutchoucs et des élastomères thermoplastiques*, Edite par Christian G'Sell et Alain Coupard (1997), pp. 351–354.
8. J. T. Tsai, "The compressive deformation of polymeric foams," *Polymer Engng. Sci.*, **22**, No. 9, 545–548 (1982).
9. S. K. Vidyarthi, "Density and strength of plastic foams," *Cellular Polymers*, **3**, No. 1, 1–9 (1984).
10. J. L. Throne, "Effect of density on compressive stress-strain behavior of uniform density closed cell foams," *J. Cellular Plastics*, May–June, 178–182 (1985).
11. L. J. Gibson and M. F. Ashby, *Cellular Solids, Structures and Properties*, Pergamon Press (1988).
12. J. P. Yvrard, *Expérimentation et modélisation du comportement mécanique du polystyrène expansé*, These Universite des Sciences et Technologies de Lille (1998).
13. C. J. Benning, *Plastic Foams: The Physics and Chemistry of Product Performance and Process Technology*. Volume I: *Chemistry and Physics of Foam Formation*, Wiley Interscience (1969).
14. C. J. Benning, *Plastic Foams: The Physics and Chemistry of Product Performance and Process Technology*, Volume II: *Structure, Properties, and Applications*, Wiley Interscience (1969).
15. J. Miltz, O. Ramon, and S. Mizrahi, "Mechanical behavior of closed cell plastic foams used as cushioning materials," *J. Appl. Polymer Sci.*, **38**, 281–290 (1989).
16. J. Sarlin, Pe. Järvelä, Pi. Järvelä, and P. Törmälä, "The inhomogeneity inside a block of expanded polystyrene (E.P.S.)," *Plastics and Rubber Processing and Applications*, **6**, No. 1, 43–49 (1986).
17. M. C. Shaw and T. Sata, "The plastic behavior of cellular materials," *Int. J. Mech. Sci.*, No. 8, 469–478 (1966).

18. I. M. Ward, and D. W. Hadley, *An Introduction to the Mechanical Properties of Solid Polymers*, Wiley Interscience (1993).
19. K. Boytard, A. Ouâkka, and K. Dang Van, "A modeling tool for the mechanical behavior of polyethylene pipe," in: *Pipeline Technology*, Vol. I, Elsevier Science (1985), pp. 245–253.
20. A. Ouâkka, K. Dang Van, D. Gueugnaut, and P. Blouet, *Etude du comportement du polyéthylène*, 3éme congrès de mécanique, Tetouan, Maroc (1997).
21. M. K. Neilsen, R. D. Krieg, and H. L. Schreyer, "A constitutive theory for rigid polyurethane foam," *Polymer Engng. Sci.*, **35**, No. 5, 387–394 (1995).

Received 24. 10. 2000